



## ORIGINAL ARTICLE

# Collaborative impact of Cu/TiO<sub>2</sub> nano composites for elimination of cationic dye from aqueous solution: Kinetics and isothermal modeling



Alaa M. Munshi

Department of Chemistry, Faculty of Applied Science, Um Al-Oura University, Makkah Province 21955, Kingdom of Saudi Arabia

Received 31 January 2023; accepted 13 March 2023

Available online 23 March 2023

## KEYWORDS

Cu/TiO<sub>2</sub> nano composites;  
Methylene blue;  
Adsorption

**Abstract** Nano TiO<sub>2</sub> is economic nano particles have many applications. This study focus on evaluation of Cu/TiO<sub>2</sub> nano composites mechanically prepared for elimination of methylene blue dye (MB) in its aqueous solutions. Two molar ratios of TiO<sub>2</sub> to Cu were used for the fabricated nano composites; (1:1)(TC1) and (2:1)(TC2). The fabricated doped particles were characterized by N<sub>2</sub> adsorption–desorption isotherm, (FTIR) and (SEM/ EDAX) techniques. The results clarify that Cu atoms were randomly covered or precipitated on TiO<sub>2</sub> nano particles resulting to increase in the porosity and surface roughness. The uptake study was conducted via batch mode under various processing parameters like pH, contact time, initial dye concentration and adsorbent mass. The results revealed that, maximum uptake 77–90 mg/g was achieved at solution pH = 5 for TiO<sub>2</sub> and pH = 7 for doped TiO<sub>2</sub> with an equilibrium time 6 h for studied samples. Removal % was in order TC1 > TC2 > T which correlated to the amount of deposited Cu in nano composites. Besides, the adsorption capacity increased by increasing the adsorbent mass and much reduced by boosting the dye concentration. This is explained due to the electrostatic interaction between benzene ring in MB and the electron cloud of Cu molecules. Pseudo 2nd order kinetic model was more appropriate to describe the adsorption of MB onto doped TiO<sub>2</sub> nano particles and the experimental data were more fitting to Freundlich model suggesting a heterogeneous adsorption.

© 2023 The Author(s). Published by Elsevier B.V. on behalf of King Saud University. This is an open access article under the CC BY-NC-ND license (<http://creativecommons.org/licenses/by-nc-nd/4.0/>).

## 1. Introduction

Water is the main need substance for life on Earth. Contamination of already present water resources by various pollutants is of the major global problem which faces all regions in Worldwide (Al Abdugader et al., 2013, Pérez-González et al., 2012). Water sources including rivers, water streams and lacks may be contaminated by organic effluent, colored dyes, heavy metals ions, nutrients and chemical pesticides. Discharge of these contaminates to aquatic environments changes both the chemical and physical properties of water as well as its biological properties. These reflected in toxicity for marine life which seriously

E-mail address: [alaamunshi933@yahoo.com](mailto:alaamunshi933@yahoo.com)

Peer review under responsibility of King Saud University.



<https://doi.org/10.1016/j.arabjc.2023.104815>

1878-5352 © 2023 The Author(s). Published by Elsevier B.V. on behalf of King Saud University.

This is an open access article under the CC BY-NC-ND license (<http://creativecommons.org/licenses/by-nc-nd/4.0/>).

affect all the life cycle (El-Asser et al., 2021). Continuously, it causes a disorder for human body as well as the other living organisms. Additionally, the physical and chemical changes in the water nature is a reason for the unbalances of water pH and death of aquatic life.

Methylene blue (MB) is a typical cationic dye, results from many industries such as paper manufacturing, painting production and glass finishing (Hashem, 2013, Hashem, 2012; Hashem and Amin, 2016, Ahmed et al., 2019, Firdaus et al., 2022). The direct contact of MB by human is harmful and may create many dangerous diseases including cancer (Pearce et al., 2003). Many technologies have been used to remove dyes pollutant from wastewater such as; electro dialysis (Van der Bruggen et al., 2003), reverse osmosis (Tepuš et al., 2009), utilization of microwave or ultrasonic waves (Collings and Gwan, 2010, Gong et al., 2011), photocatalytic degradation (Katsumata et al., 2011), ozonation, and adsorption (Hashem and Amin, 2016, El-Shafei et al., 2009). Adsorption represents an ease, low cost and an effective method for elimination of many pollutants from aqueous medium (Memon et al., 2014). Activated carbon, algae, palm, seeds residue and bagasse-bentonite are examples of low cost adsorbent had been used as effective removal for many organic pollutants, dyes, pesticides or heavy metals (Kuncoro et al., 2018a, 2018b, Kheraa et al., 2020, Neolaka et al., 2023).

Recently many researchers recommended the application of nanoparticles in the wastewater treatment as an effective and low-cost technology (Elzain et al., 2019, Firdaus et al., 2023). Different attempts were carried out to prepare nano particles or nano fibers to be used for the wastewater treatment (Elkady et al., 2020). Nano particles have many innovative and basic properties such as; the extremely small size, an excellent absorption features, and a highly chemical reactivity and selectivity (Elzain et al., 2019, Marcilin et al., 2014). So, nano adsorbents are most appropriate for remediation of metal ions, organic and inorganic pollutants from wastewater (Sushma and Richa, 2015, Monteiro-Riviere et al., 2011).

Due to its safety-use, scalability and economic cost; TiO<sub>2</sub> has a wide application in many industrial fields (Pichot et al., 2000, Veréb et al., 2012). Nano TiO<sub>2</sub> is an effective catalyst for photo degradation under UV- irradiation of many pollutants especially ploy cyclic aromatic hydrocarbons (PAH) and azo-dyes. (Yu et al., 2005, Shahmoradi et al., 2010). TiO<sub>2</sub> NPs are a semiconductor with a 3.2 eV wide bandgap for anatase and 3.0 eV for rutile (Nabi et al., 2020, Araujo et al., 2020, Pascariu et al., 2021). However, Due to its fine particles, TiO<sub>2</sub> NP makes a white suspension with water which cannot be removed by filtration. So TiO<sub>2</sub> NP cannot be used directly with water for treatment of wastewater. NanoTiO<sub>2</sub> can be supported into another solid such as another metal (Basnet et al., 2019) or loaded on nanofibers Lazar et al., 2012) or clays (De Oliveira et al., 2020, Araujo et al., 2020). Doping of TiO<sub>2</sub> nano particles by another metal causes surface modifications that can diminish the band gap of the catalyst and expedite the light absorption in the visible region (Ziemkowska et al., 2014, McDonald et al., 2015). CuO nano particles are used to remove arsenic from groundwater (Miao et al., 2017) and biofilms (Narayana et al., 2011) while copper in its nano form has the activity to control the microorganism's reproduction and remediation of heavy metals (Abazović et al., 2006).

In the present study, economic TiO<sub>2</sub>-doped Copper nano particle were simply manual synthesized and characterized. Batch experiments were carried out to explore the elimination efficiency of Cu/TiO<sub>2</sub> doped nano particles towards methylene blue dye from wastewater. MB was used as an example of one of abundant pollutant can be found in wastewater and results from many industries. The kinetics and thermodynamics of the removal process were investigated.

## 2. Experimental protocols

### 2.1. Chemicals

Ti(IV) dioxide (Anatase) nano particles was supplied from Sigma-Aldrich with particle size  $\leq 25$  nm (purity  $> 98$  %,

density 0.04–0.06 g/ml). The surface characterization of TiO<sub>2</sub> nano particles were analyzed by N<sub>2</sub>-adsorption isotherms at 77 K using volumetric instruments connected to a vacuum for outgassing until reach 10–5 Torr. Copper metal powder (lobachemie, purity  $> 96$  %) was used as doped metal in nano titanium dioxide. Methylene blue (MB) dye of molecular formula C<sub>16</sub>H<sub>18</sub>ClN<sub>3</sub>S, molar mass 319.85 g/mol, was supplied by Merck (Mumbai, India). Standard stock solutions of methylene blue dye (MB) were prepared by dissolving a certain amount of the pollutant in distilled water to get 1000 ppm of MB solution. Dilution was carried out to get different concentrations of dye solutions. NaOH and HCl (Sigma-Aldrich) were used for adjusting the solutions pH.

### 2.2. Preparation of Cu/TiO<sub>2</sub> nanoparticles

First, TiO<sub>2</sub> nano particles was thermally activated at 200 °C for 4 h. Cu/TiO<sub>2</sub> doped nano particles was prepared simply by mechanical mixing of copper powder with TiO<sub>2</sub> nano particles in two molar ratios 1:1 and 2:1 (TiO<sub>2</sub>: copper). These mixtures were manually grinded carefully using a mortar and pestle for 1 hr. After mixing, the samples were placed in porcelain crucibles and heated at 200 °C for 12 hrs. Symbols T, TC1 and TC2 were taken to designate undoped TiO<sub>2</sub>, doped copper: TiO<sub>2</sub> (1:1) and (2:1) respectively. TiO<sub>2</sub> and TiO<sub>2</sub> doped nano particles were characterized using an automatic surface area and pore size analyzer (BELSORP MINI X) via adsorption-desorption of N<sub>2</sub> gas at 77 K. Fourier transform infrared spectrometer (BIO-RAD FTS-40) and Scanning Electron microscope (SEM) images were observed for the doped samples using SEM (JEOL JSM6360LA, Japan) at an accelerated voltage of 10 kV combined with energy dispersive X-ray spectroscopy (EDX, Oxford 7021) for the determination of elemental composition.

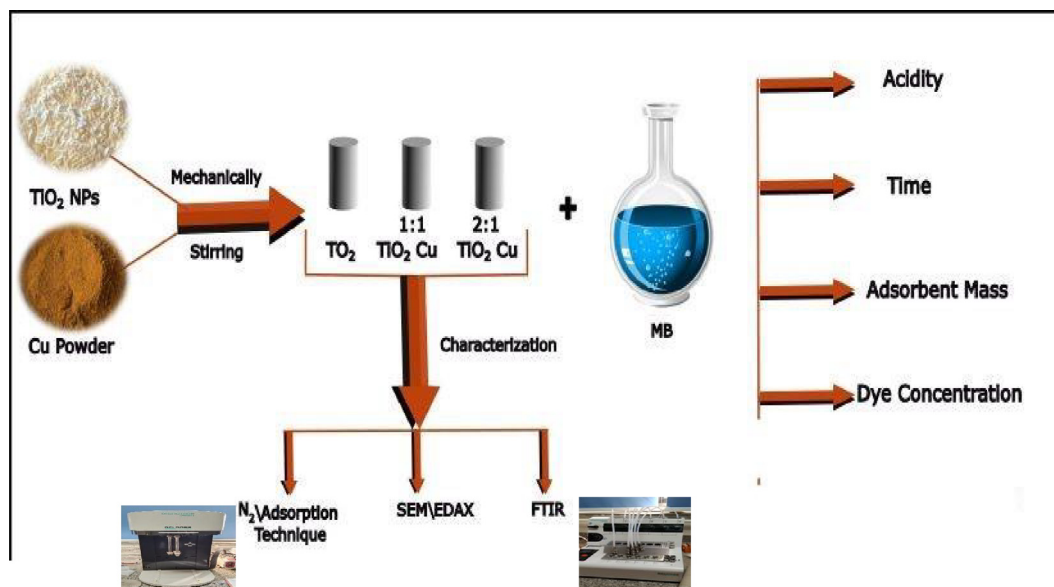
### 2.3. Dye uptake experiments

Batch experiments were adopted for studying the elimination characterization of methylene blue by Cu/TiO<sub>2</sub> doped nano particles from aqueous medium. The influence of the processing batch parameters such as contact time (0.5, 1.5, 2, 6, 12, and 24 h); pH (2, 5, 7, 10, and 12); dye concentration (10, 20, 50, 100 and 200 mg/l) and the doped sample dosage (0.01, 0.02, 0.035 and 0.05 g) were investigated. Each batch experiment was performed in 50 ml beaker covered with aluminum foil and the dye solution (containing the doped nano particles), and then the solution was magnetically stirred (150 rpm) at 25 °C. The remaining dye concentration in the filtrate was determined by using UV-spectrophotometer (Spectord 200) at wavelength = 668 nm. For each experiment. The solution pH was measured using Hanna model pH sensor. Each experiment was done two replicates and the average value was recorded.

The removal percent (R%) was calculated using Eq. (1) and the uptake capacity of MB (mg/g) by Eq. (2);

$$R\% = \frac{C_0 - C_e}{C_0} \times 100 \quad (1)$$

$$qe = \frac{(C_0 - C_e)V}{m} \quad (2)$$



**Scheme 1** Methodology for preparing Cu/TiO<sub>2</sub> composite, and the studied parameters for removal of MB.

Where;  $C_0$  and  $C_e$  are the initial concentration (mg/l) and equilibrium concentration of MB in the solutions,  $V$  the volume of the solution (L), and  $m$  is the mass (g) doped nano particles used in the removal process.

**Scheme 1** shows the experimental procedures for Cu/TiO<sub>2</sub> preparation, characterization and MB elimination tests.

### 3. Results and discussion

#### 3.1. Characterization of TiO<sub>2</sub> and Cu/TiO<sub>2</sub> nano particles

Surface characteristics and pore volumes of nano TiO<sub>2</sub> (sample T) were studied using an automatic surface area and pore size analyzer (BELSORP MINI X) via adsorption-desorption of N<sub>2</sub> gas at 77 K. The classified as type II with very minor H1 hysteresis loop according to IUPAC classifications (Nabi et al, 2020, Gayathri et al, 2019). The texture characteristics were,  $S_{BET}$  area (87 m<sup>2</sup>/g), total pore volumes  $V_p$  (0.0616 cm<sup>3</sup>/g), average pore diameter (28.3 nm) and monolayer capacity  $V_m$  equals 2.0 cm<sup>3</sup>/g; Such data confirms the macro pores through packing of nano-TiO<sub>2</sub> particles packing microporosities nature of the prepared nano TiO<sub>2</sub> (Fig. 1).

Fig. 2a-c show SEM images of T, TC1 and TC2 samples. TiO<sub>2</sub> nano particles appeared as micro spherical particles with diverse size distribution with diameter ranged between 20 and 80 nm, a histogram of particle size distribution of TiO<sub>2</sub> nanoparticles is shown in Fig. 2d. SEM images of doped samples (TC1 and TC2) show a fine agglomerate of abundant spherical particles of TiO<sub>2</sub> nano particles in which Cu clusters are precipitated and/or covered. This inhomogeneity in the distribution of Cu particles on NT surfaces resulting in a surface roughness with creation of more active sites, see Fig. 2b & c. Energy-dispersive X-ray spectroscopy (EDAX) of doped samples illustrate presences of O, Ti and Cu with atomic stoichiometric of 64.77, 08.96 and 25.18% for TC1 and 64.77, 18.02 and 16.95 for TC2 respectively, Fig. 3 (Some traces of Al were appeared in EDAX images of TC1 and TC2 due to possible

contamination during preparation of these two composites or during doing the EDAX test.

FTIR spectrum of TiO<sub>2</sub> nano particles; Fig. 4, shows two main bands. The first broad band is observed at 3450 cm<sup>-1</sup>, corresponding to the stretching vibration of the hydroxyl group O—H of the TiO<sub>2</sub>. The second band is observed around 1630 cm<sup>-1</sup>, owing to bending modes of H—O—H bond of physically absorbed water. The same bands are observed for Cu/TiO<sub>2</sub> (1:1) doped nano particles but with diminished intensities. This could be related to the possibility of attachment of copper by TiO<sub>2</sub> through Cu substitution the hydrogen in Ti—O—H bond to form Cu—O bond (Mugundan et al 2015, Sadanandam et al 2013, De Oilveria et al, 2020). After uptake of methylene blue dye by Cu/TiO<sub>2</sub> (1:1) doped nano particles, FTIR spectrum shows disappearances of all the band related to O—H and H—O—H indicating the attachment of the organic dye by these function groups.

#### 3.2. Factors affecting dye uptake process

##### 3.2.1. Effect of pH

In general, the initial pH of the removal solution can enhance or depress the rate of dye uptake besides it is highly correlated with changes in the adsorbent surface and dye ionization (Foo and Hameed, 2010). Fig. 5 demonstrates the variation of removal percent (R%) for samples T, TC1 and TC2 with the pH of dye solution. The removal conditions were 50 ml solution containing 0.05 g of adsorbent, 100 mg of dye and contact time 6 h with initial solution pH 2–12. pH was adjusted by using standard solutions of NaOH or HCl before adding the solid adsorbent. The results showed that for all studied samples; the removal percent of MB was pH-dependent as well as it related the atomic % of doping Cu in the nanocomposites which inconvenient to the EDAX data given in section 3.1. Sample T (TiO<sub>2</sub> before doping) demonstrates R% (59%) at pH = 5 while the doped samples (TC1 and TC2) offer high removal percent (80 % and 62% respectively) at pH = 7.

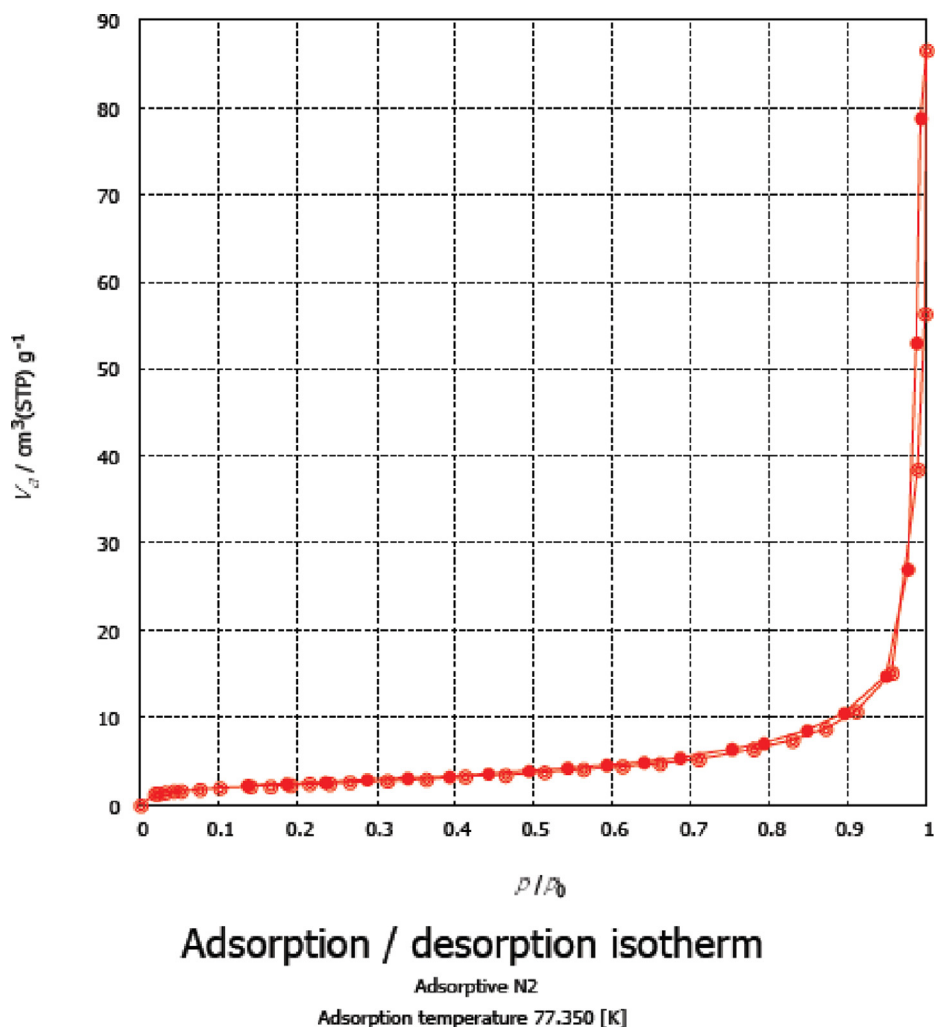


Fig. 1 Adsorption-desorption isotherm of sample T.

The reduced removal of MB at acidic pH owing to the presence of excess proton ( $H^+$ ) ions competing with MB cations for the available active sites or sorption spots (Ali et al 2019, Foo and Hameed, 2010, El-Aassar et al 2022). Besides, at low pH, there is a repulsion between the protonated surface sites on the nano adsorbents and the protonated dimethyl amine group in MB which will reduce R% values (El-Aassar et al 2021). Another explanation is the possible reduction of MB into  $MBH_2^+$  at pH 2–7 (Sohrabnezhad et al, 2010) which hinder its interaction with the active sites of the nanocomposites. Boosting pH of the solution results in deprotonation of the sorption sites on the surface, thus the surface becomes negatively charged with high attractive properties to the MB (Hashem 2013). At alkaline pH all the sites were deprotonated caused an increase in the electron cloud and thus, the repellent forces increased (Elzain et al 2019, Sadanandam et al 2013).

During the uptake experiment, initial pH of the solution could change, Fig. 6 demonstrates the pH variation ( $\Delta pH$ ) before and after MB dye elimination at various initial solutions pH. At acidic  $pH \leq 5$ , there is an increase in the pH of the dye solution after elimination process (solution become more basic) due to strongly sorption of ( $H^+$ ) on expense of

the sorption of MB molecules. While at neutral to relatively basic medium, the available negatively charged sites increased leading to highly attracted the cationic MB resulted in unchange or slightly reduce the solution pH after the removal process. At  $pH \geq 10$  all the surface sites became deprotonated and the sorption of MB associated by decreasing in pH of the solution (solution become more acidic). pH 5 was conducted as optimum solution pH for T sample while  $pH = 7$  was chosen for TC1 and TC2 doped samples.

### 3.2.2. Effect of contact time

Contact time is an important parameter that determine the efficiency of the eliminating materials and its application befit. The elimination behavior (R%) of MB dye by T, TC1, and TC2 is studied in duration time up to 24 h ( $pH = 7$ , 0.05 g of adsorbent and 100 mg of MB) and it is demonstrated in Fig. 7. The results reveal that, the studied samples showed a comparable fast rate of MB removal at the initial contact time and about 50% of the dye were eliminated after the first 6 h for the three studied samples. From 6 to 24 h, the removal rate diminished and nearly an equilibrium state is reached at 24 h. During the initial contact time, most of the vacant sur-

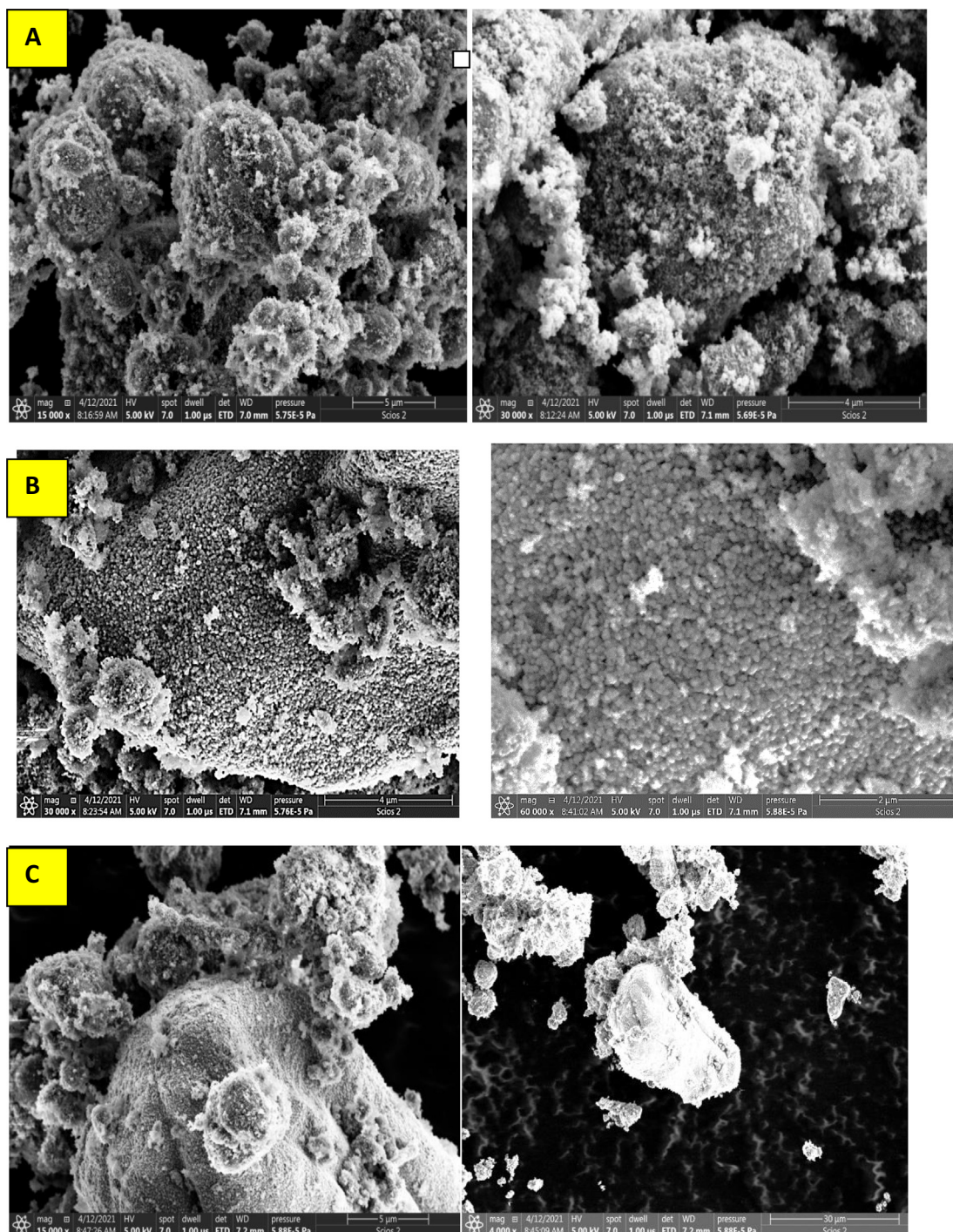
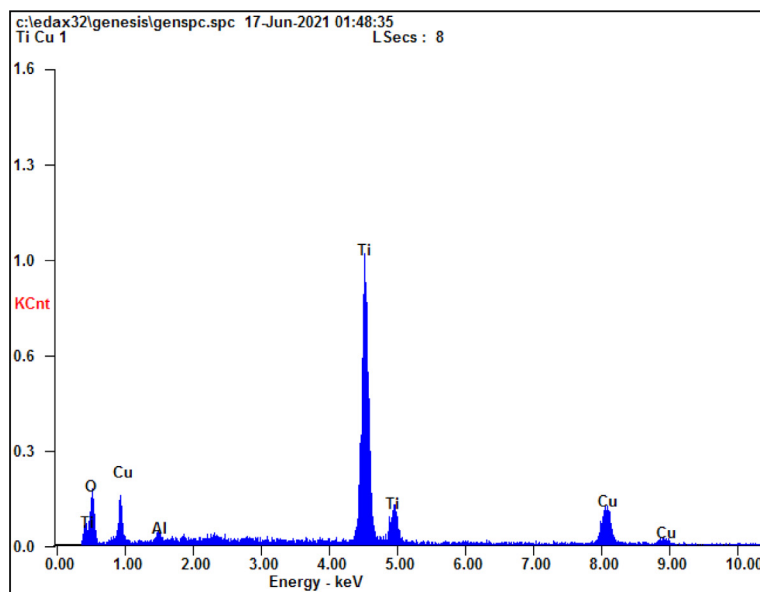


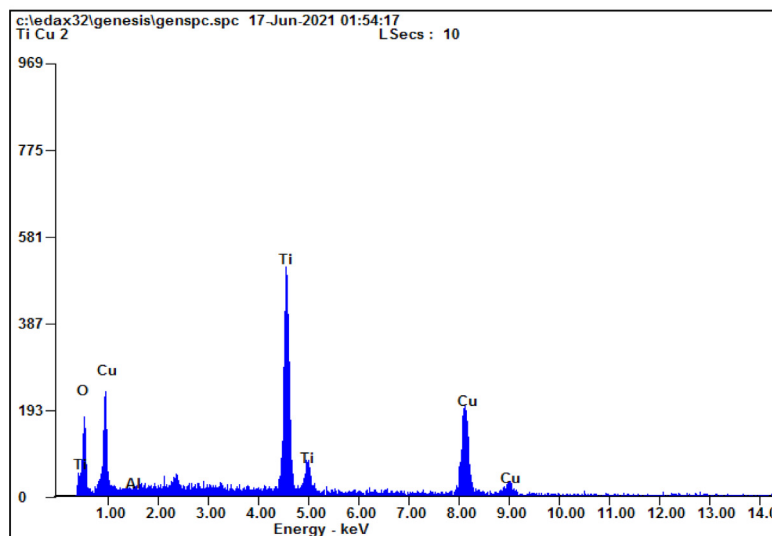
**Fig. 2** SEM images of A)T, B)TC1 and C)TC2 samples.

face sites were available for MB cations, facilitates the diffusion of the dye molecules from the solution bulk to the interior surface and hence to available sites. So, the rate of dye elimination became fast. At later times, the fraction of available active sites was diminished due to their blocking by the adsorbed dyes which resist the dye diffusion and as a sequence rate of dye elimination was reduced (Hashem, 2013, [El-Aassar et al 2022](#)). (R%) were 86, 62 and 57 for TC1, TC2 and T respectively in a relation to the % of the deposited Cu on the nano

composites, see EDAX results in [section 3.1](#). Depositing of Cu atoms on TiO<sub>2</sub> nano particles results to many possible actions (i) boosting of surface area and as a sequence the number of active sites in the doping composites. (ii) A possible electrostatic interaction between benzene ring in MB and the electron cloud of Cu molecules via  $\pi$ - $\pi$  bonding +/or Van der Waal forces leading to more elimination percent. 6 h. is adopted as optimum contact times for the three studied samples which is comparable to those recorded by another adsorbents whose



Element	Wt %	At %
O K	35.98	64.07
AlK	01.69	01.79
TiK	42.34	25.18
CuK	19.98	08.96



Element	Wt %	At %
O K	34.74	64.77
AlK	00.23	00.25
TiK	28.93	18.02
CuK	36.10	16.95

Fig. 3 EDAX elemental analysis of TC1 & TC2 samples.

reported earlier in literature (El-Aassar et al 2022, Firdaus et al, 2023).

### 3.2.3. Effect of MB initial concentration

The initial dye concentrations afford a vital power to overcome the facing resistance of the mass transfer of the dye molecules. The removal of MB dye was conducted at different dye concentrations (10–200 mg/L) (pH = 7, 0.05 g of adsorbent, contact time 6 h) as shown in Fig. 8. As shown, increasing the MB concentration resulted in a reduction in the R% by all the studied samples. Reduction in R % was significant by increasing the dye concentration from 10 to 100 mg (R% diminished by 3 fold), while from 100 to 200 mg, no significant reduction in R% was noted. Low dye concentration was associated with low repulsion between MB molecules and high dif-

fusion of MB from the aqueous phase to the external solid adsorbent phase (Hashem and Amin 2016, El-Aassar et al 2022). Additionally, the overcrowding of adsorbent particles among the adsorption sites at high dye contents reduces the uptake capacity (Haque et al 2010). The order of removal in sequence TC2 > TC1 > T revealing doping composites over more active sites which offers more removal efficiency.

### 3.2.4. Effect of adsorbent dose

Fig. 9 represents the variation R% with the adsorbent mass (0.0 – 0.05 g) (pH = 7, 100 mg MB, contact time 6 h). Here, R % for T, TC1 and TC2 increases continuously by boosting the adsorbent dose in the removal solution. About 98, 87 and 65% of the dye were removed using adsorbent mass 0.05 g. Increasing the amount of nano particles (doped or non-

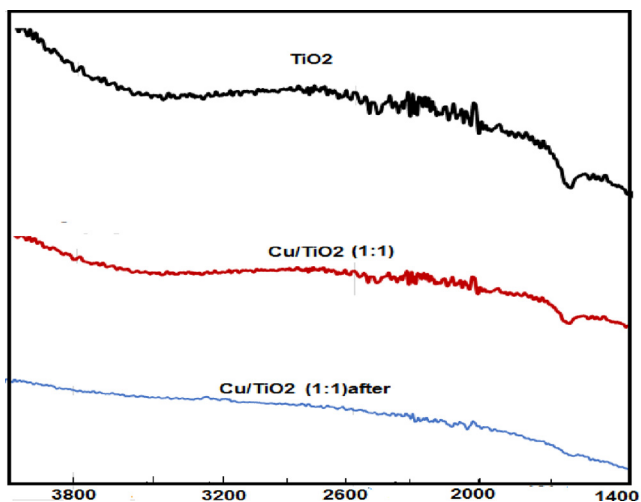


Fig. 4 FTIR spectrum of TiO<sub>2</sub> nano particles, TC1 and TC1 after elimination of MB.

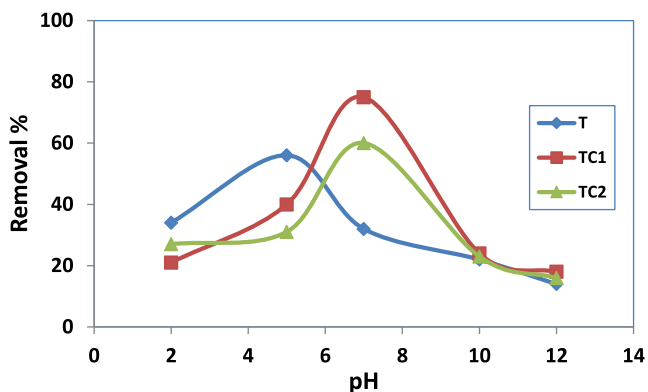


Fig. 5 Effect of pH on R% of MB by T, TC1 and TC2.

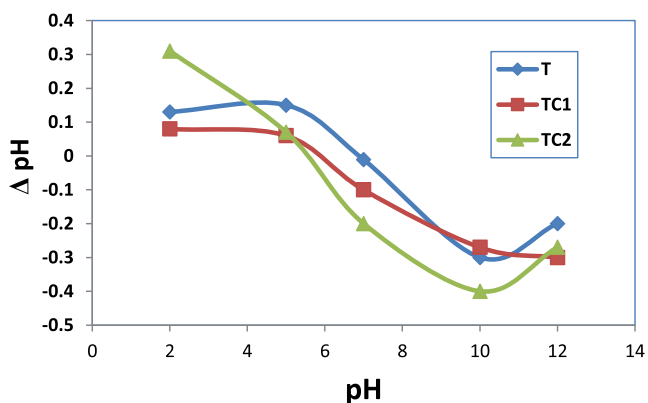


Fig. 6 Variation of pH ( $\Delta$  pH) with initial pH solution for T, TC1 and TC2.

doped) affords more surface area with more available active sites, So it gradually promotes the MB removal efficiency (El-Aassar et al 2019). Similar results was reported for M.B using graphene oxide by liu et al.(Liu et al., 2012) whose

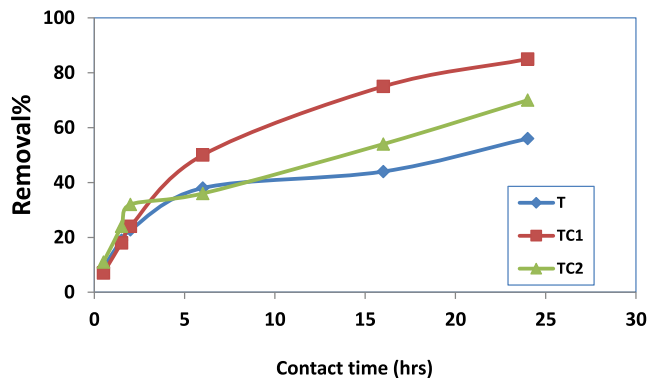


Fig. 7 Effect of contact time on R% of MB by T, TC1 and TC2.

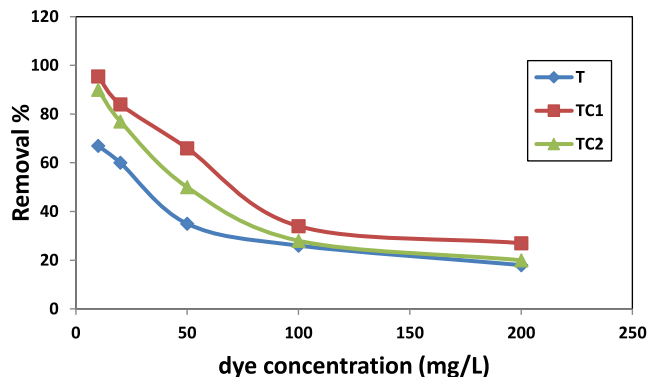


Fig. 8 Effect of dye concentration on R% of MB by T, TC1 and TC2.

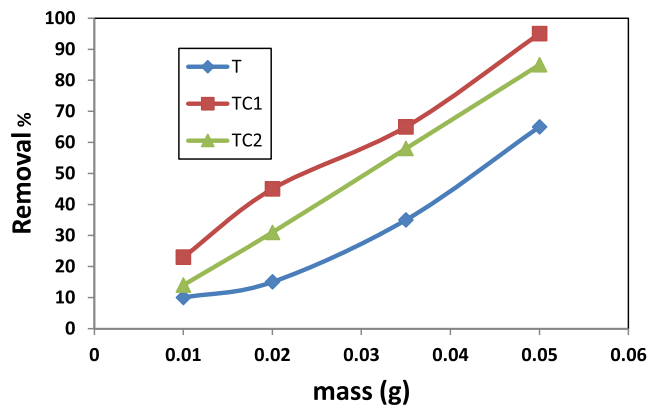


Fig. 9 Effect of adsorbent dose on R% of MB by T, TC1 and TC2.

related that increasing sorbent dose enhances the driving diffusion force for elimination.

### 3.3. Kinetics of MB elimination

Pseudo 1st order, pseudo 2nd order and intra-particles models were tested for the experimental data of elimination of MB on samples T, TC1 and TC2. The linear form of pseudo 1st order and 2nd kinetic models are expressed as Eqs. (3)&(4):

$$\ln(q_e - q_t) = \ln q_e - k_1 t \quad (3)$$

$$t/q_t = 1/k_2 q_e^2 + t/q_e \quad (4)$$

Where;  $q_e$ : the concentration of MB eliminated at equilibrium,  $q_t$ : the concentration of MB eliminated at time (t),  $k_1$  ( $\text{hrs.}^{-1}$ ) is pseudo 1st order rate constant;  $k_2$  ( $\text{g/mg h}$ ) is pseudo 2nd order rate constant which can be computed from the intercept of the straight line obtained from plotting  $t/q_t$  vs. t.

Intra-particle diffusion model (IPD) is expressed in (Eq. (5)):

$$q_t = K_d t^{1/2} + C \quad (5)$$

Intra-particle diffusion model assumes the transport of MB ions from the aqueous solution to the surface of adsorbents is controlled by diffusion forces then followed by the transfer of the MB molecules into the interior pores of nano sorbent.  $C$  ( $\text{mg g}^{-1}$ ) and  $K_d$  ( $\text{mg/g.hr}^{-1/2}$ ) are constants were evaluated from the slope of the linear fraction of the curve between  $q_t$  against  $t^{1/2}$ .

The best-fit mechanism is determined depending on the linear correlation coefficient ( $R^2$ ) values. The constants were shown in Table 1 and pseudo 1st and 2nd plots were represented in Figs. 10a and 10b respectively.  $R^2$  values of the pseudo 2nd order rate were = 0.966, 0.999 and 0.980 for T, TC1 and TC2 respectively. This proves that the elimination process of MB by nano  $\text{TiO}_2$  and  $\text{Cu/TiO}_2$  doped nano particles can be expressed well by the pseudo 2nd order kinetics mechanism (Hashem, 2013, Patrick 1995).

Fig. 10c shows the linear plot of intra-particles diffusion model. Due to high  $R^2$  values (0.948, 0.983 and 0.957 for T, TC1 and TC2 respectively) it can be demonstrated that IPD played a significant role in the uptake of MB by the three nano sorbents especially at the early time duration of the uptake process. Additionally, the value of  $C$  gives a prediction about the thickness of the boundary layer. However, the three plots of IPD models did not pass through the origin meaning that, the diffusion mechanism was not the sole rate-controlling step and the elimination of MB onto the adsorbent was a multi-step process with the possibility of chemisorptions and H-H bonding formation among MB molecules and surface sites. To investigate that, Elovich model was examined for the experimental data, which can be represented in Eq. (6):

$$qt = \alpha + \beta \ln t \quad (6)$$

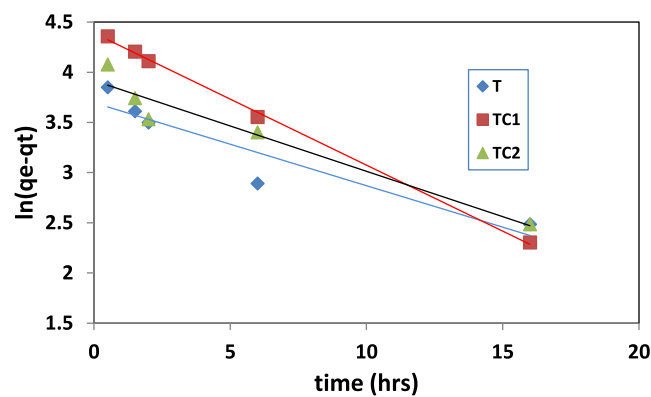


Fig. 10a Linear plot of pseudo 1st order rate model.

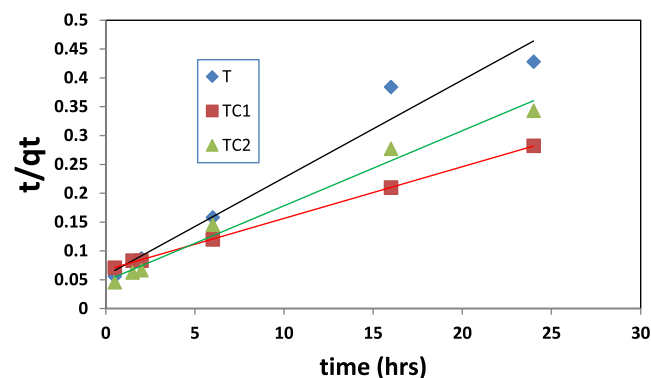
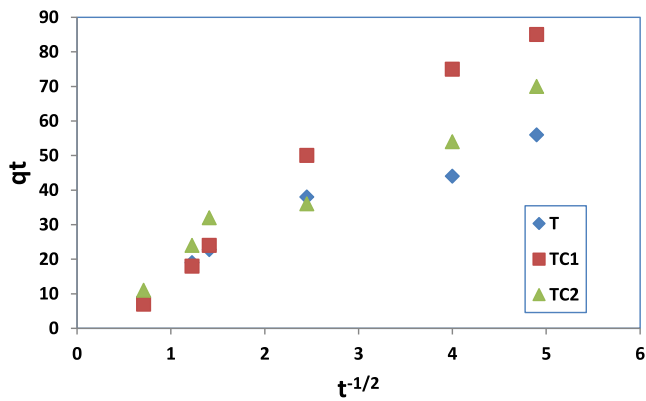


Fig. 10b Linear plot of pseudo 2nd order rate model.

The linear plot of Elovich model was constructed by plot  $qt$  versus  $\ln t$ . The Elovich parameters is shown in Table 1. According to the value of  $R^2$ , Elovich model showed a satisfactory fitness to the obtained experimental data of M.B sorption onto T, TC1 and TC2 samples. This confirms the chemisorptions of MB via hydrogen bonding between H-atom of OH group in nano adsorbents and the nitrogen atom in MB and/or a possible chelation between copper atom in the doped nano sorbents (TC1 & TC2) and the N-atoms in MB molecules. These results in coincidence with other reported data for M. B adsorption process (Wu and Qu 2005, Bulut and Aydın 2006, Üner et al 2016). According to these results, the

Table 1 Kinetic parameters for adsorption of MB onto T, TC1 and.

Model	Parameters		
	T	TC1	TC2
Pesudo 1st order rate equation	$R^2 = 0.883$ $K_1(\text{h.}^{-1}) = 0.082$	$R^2 = 0.986$ $K(\text{h.}^{-1}) = 0.131$	$R^2 = 0.936$ $K(\text{h.}^{-1}) = 0.090$
Pesudo 2nd order rate equation	$R^2 = 0.966$ $K_2 = 0.0045(\text{g/mg.h})$ $q_{e, \text{cal.}} = 62.5 (\text{mg/g})$ $q_{e, \text{exp.}} = 60 (\text{mg/g})$	$R^2 = 0.999$ $K_2 = 0.0137(\text{g/mg.h})$ $q_{e, \text{cal.}} = 85 (\text{mg/g})$ $q_{e, \text{exp.}} = 90 (\text{mg/g})$	$R^2 = 0.984$ $K_2 = 0.01297(\text{g/mg.h})$ $q_{e, \text{cal.}} = 60 (\text{mg/g})$ $q_{e, \text{exp.}} = 77 (\text{mg/g})$
Intra-particle diffusion model	$R^2 = 0.948$ $K_d(\text{mg/g t}^{1/2}) = 10.2C = 6.4$	$R^2 = 0.9824$ $K_d(\text{mg/g}^{-1/2}) = 19C = 3.2$	$R^2 = 0.957$ $K_d(\text{mg/g t}^{1/2}) = 12.3C = 7.5$
Elovich model	$R^2 = 0.968$ $\alpha = 0.353(\text{mg/g.h}) = 3.04$ $(\text{mg/g})\beta$	$R^2 = 0.977$ $\alpha = 0.548(\text{mg/g.h}) = 2.98$ $(\text{mg/g})\beta$	$R^2 = 0.962$ $\alpha = 0.356(\text{mg/g.h}) = 2.78$ $(\text{mg/g})\beta$



**Fig. 10c** Linear plot of intra particle diffusion model.

pseudo-2nd order and Elovich models with respect to the intra particles diffusion mechanism are adopted to be the most fitting models for describing the MB uptake process onto the three nano adsorbents.

### 3.4. Adsorption isotherm

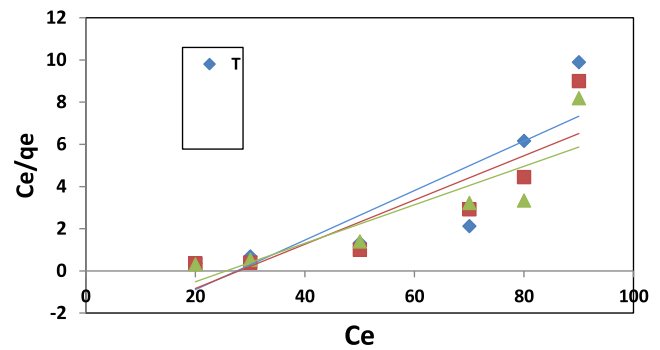
To understand the interaction mechanisms between MB onto T, TC1 and TC2 samples. Freundlich and Langmuir isothermal models were applied to experimental data which they are expressed in Eqs. (7) and (8) respectively.

$$\ln q_e = \ln K_f + 1/n \ln C_e \quad (7)$$

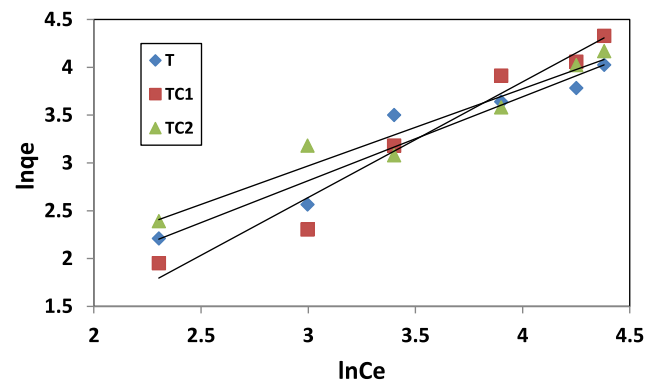
$$C_e/q_e = 1/bq_m + C_e/q_m \quad (8)$$

Where:  $K_f$  and  $n$  are Freundlich constants that determines the sorption divergence or surface heterogeneity;  $C_e$  (mg/l) is the equilibrium concentration,  $q_e$  (mg/g) is the amount adsorbed,  $q_m$  (mg/g) and  $b$  (l/mg) is the Langmuir constants that they refer to maximum adsorption performance and binding energy, respectively. The isotherm parameters and the correlation coefficients are presented in Table 2 and the linear plots are shown in Fig. 11a & b.

The two adsorption isotherms are constructed by plotting  $C_e/q_e$  versus  $C_e$  for Langmuir and  $\ln q_e$  versus  $\ln C_e$  for Freundlich. The correlation coefficients ( $R^2$ ) determine the most related model to the adsorption process. The values of  $R^2$  for Langmuir (0.748, 0.774 and 0.764) and Freundlich (0.928, 0.960 and 0.947) for T, TC1 and TC2 respectively indicating the equilibrium data are in good fitting with the Freundlich isotherm. This assumes the elimination of MB by



(a)



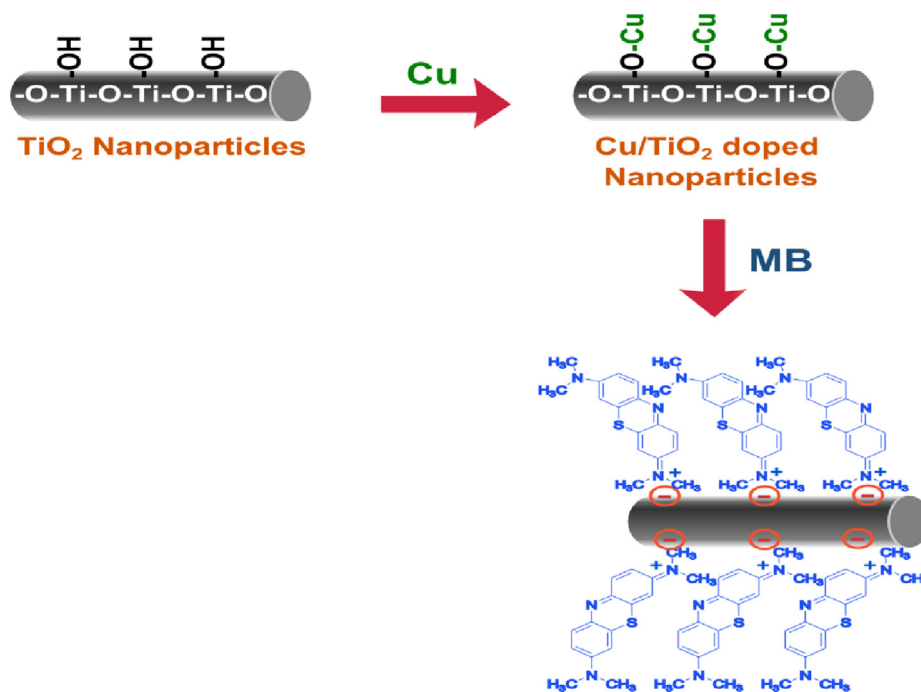
(b)

**Fig. 11** Linear plots of various isothermal models a) langmuir b) freundlich.

nano adsorbents is a divergence adsorption on heterogeneous surfaces (Elkady et al 2016). Scheme 2 shows a presentation of the interaction mechanisms of MB onto nano adsorbents. The achieved capacity in our work is relatively high (60–90 mg/g) compared with other natural or artificial sorbents which were reported earlier in the literature for examples: activated carbon (9.81 mg/g) (Bulut and Aydm 2006), Kaolin with graphene oxide (28.02 mg/g) (He et al 2018), Zeolite (22.0 mg/g) (Rida et al 2013), poly (styrene-co-acrylonitrile) nanofibers (7.3 mg/g) (Elzain et al 2019) cellulose nanofibers (49.5 mg/g) (Ali et al 2019) modified cellulose (55.04 mg/g) (dos Santos Silva et al 2018).

**Table 2** Isothermal models for adsorption of MB onto T, TC1 and TC2.

Isotherm	Parameters	T	TC1	TC2
Langmuir	$R^2 = 0.748$ $q_m = 15.65$ (mg/g) $b = 3.1$	$R^2 = 0.774$ $q_m = 19.62$ (mg/g) $b = 3.4$	$R^2 = 0.764$ $q_m = 10.98$ (mg/g) $b = 4.3$	
Freundlich	$R^2 = 0.928$ $1/n = 0.877$ $K_f = 1.198$ (mg/g)	$R^2 = 0.961$ $1/n = 1.21$ $K_f = 0.371$ (mg/g)	$R^2 = 0.947$ $1/n = 0.806$ $K_f = 2.58$ (mg/g)	



**Scheme 2** A presentation of the interaction mechanisms of MB onto Cu/TiO<sub>2</sub> doped nano particles.

#### 4. Conclusions

According to our study the following outcomes can be driven:

- 1- Doping of TiO<sub>2</sub> nano particles by copper particles increases the roughness of the surface which achieved high elimination behavior than TiO<sub>2</sub> nano particles.
- 2- The maximum uptake 77–90 mg/g were achieved at solution pH = 7 for doped nanocomposites and equilibrium time of 6 h.
- 3- Removal % was in order TC1 > TC2 > T which correlated to the amount of deposited Cu in nano composites.
- 4- This is explained due to the electrostatic interaction between benzene ring in MB and the electron cloud of Cu molecules.
- 5- Pseudo 2nd order kinetic model is more appropriate to describe the adsorption process
- 6- The mechanism of the uptake process was found to be chemisorption according to Elovich model with respect to intra-particle diffusion process. The experimental data were more fitting to Freundlich model suggesting a heterogeneous adsorption.
- 7- Cu/TiO<sub>2</sub> doped nano particles can be considered as an effective adsorbent for MB elimination from aqueous medium.

#### Declaration of Competing Interest

The author declares that they have no known competing financial interests or personal relationships that could have appeared to influence the work reported in this paper.

#### References

- Abazović, N.D., Čomor, M.I., Dramićanin, M.D., Jovanović, D.J., Ahrenkiel, S.P., Nedeljković, J.M., 2006. Photoluminescence of anatase and rutile TiO<sub>2</sub> particles. *J. Phys. Chem. B* 110 (50), 25366–25370.
- Al Abdulgader, H., Kochkodan, V., Hilal, N., 2013. Hybrid ion exchange–Pressure driven membrane processes in water treatment: a review. *Sep. Purif. Technol.* 116, 253–264.
- Ali, A.S., El-Aassar, M., Hashem, F., Moussa, N., 2019. Surface modified of cellulose acetate electrospun nanofibers by polyaniline/β-cyclodextrin composite for removal of cationic dye from aqueous medium. *Fibers Polym.* 20 (10), 2057–2069.
- Araujo, F.P., Honorio, L.M.C., Lima, I.S., Trigueiro, P., Almeida, L.C., Fehinec, P.B.A., Santosa, F.E.P., Peña-Garcia, R., Silva-Filho, E.C., Osajima, J.A., 2020. New composite TiO<sub>2</sub>/natural gums for high efficiency in photodiscoloration process. *Ceram. Int.* 46 (10), 15543.
- Basnet, P., Anderson, E., Zhao, Y., 2019. Hybrid Cu<sub>x</sub>O–TiO<sub>2</sub> nanopowders prepared by ball milling for solar energy conversion and visible-light-induced wastewater treatment. *ACS Appl. Nano Mater.* 2, 2446–2455.
- Bulut, Y., Aydın, H., 2006. A kinetics and thermodynamics study of methylene blue adsorption on wheat shells. *Desalination* 194 (1–3), 259–267.
- Collings, A., Gwan, P., 2010. Ultrasonic destruction of pesticide contaminants in slurries. *Ultrason. Sonochem.* 17 (1), 1–3.
- De Oliveira, W.V., Morais, A.I.S., Honorio, L.M.C., Trigueiro, P.A., Almeida, L.C., Garcia, R.R.P., Viana, B.B., Furtinia, M., Silva-Filho, E.C., Osajima, J.A., 2020. TiO<sub>2</sub> immobilized on fibrous clay as strategies to photocatalytic activity. *Mater. Res.* 23 (1), e20190463.
- Dos Santos Silva, L., de Oliveira, J., Carvalho, R., de Sousa Bezerra, D., da Silva, M., Ferreira, F., Osajima, J., da Silva, E., Filho, 2018. Potential of cellulose functionalized with carboxylic acid as biosorbent for the removal of cationic dyes in aqueous solution. *Molecules* 23, 743.
- El-Aassar, M., Hassan, H., Elkady, M., Masoud, M., Elzain, A., 2019. Isothermal, kinetic, and thermodynamic studies on copper adsorption on modified styrene acrylonitrile copolymer. *Int. J. Environ. Sci. Technol.* 16 (11), 7037–7048.
- El-Aassar, M.R., Mohamed, F.M., Alsohaimi, I.H., Khalifa, R.E., 2021. Fabrication of novel valorized ecofriendly olive seed residue/anthracite /chitosan composite for removal of Cr (VI): kinetics,

- isotherms and thermodynamics modelling. Cellulose. <https://doi.org/10.1007/s10570-021-03963-y>.
- El-Aassar, M.R., Ibrahim, O.M., Hashem, F.S., Ali, A.S., Elzain, A., Mohamed, F.M., 2022. Fabrication of Polyaniline@ $\beta$ -cyclodextrin nanocomposite for adsorption of carcinogenic phenol from wastewater. *ACS Appl. Bio Mater.* 5, 4504–4515.
- Elkady, M.F., El-Aassar, M.R., Hassan, H.S., 2016. Adsorption profile of basic dye onto novel fabricated carboxylated functionalized co-polymer nanofibers. *Polymers* 8 (5), 177.
- Elkady, M.F., Salama, E., Amer, W.A., Ebeid, E., Aayed, M.M., Shokry, H., 2020. Novel eco-friendly electrospun nonmagnetic zinc oxide hybridized PVA/alginate/chitosan nanofibers for enhanced phenol elimination. *Environ. Sci. Pollut. Res.* 27, 43077–43092.
- ElShafei, G.S., Nasr, I., Hassan, A.S., Mohammad, S., 2009. Kinetics and thermodynamics of adsorption of cadusafos on soils. *J. Hazard. Mater.* 172 (2–3), 1608–1616.
- Elzain, A.A., El-Aassar, M., Hashem, F., Mohamed, F., Ali, A.S., 2019. Removal of methylene dye using composites of poly (styrene-co-acrylonitrile) nanofibers impregnated with adsorbent materials. *J. Mol. Liq.* 291, 111335.
- Firdaus, M.Y.M., Aziz, A., Azmier, A., M., 2022. Conversion of teak wood waste into microwave-irradiated activated carbon for cationic methylene blue dye removal: optimization and batch studies. *Arab. J. Chem.* 15, 104081.
- Firdaus, M.Y.M., Jaya, M.A.T., Idris, I., Abdullah, A.Z., Ahmad, M. A., 2023. Optimization and mass transfer simulation of remazol brilliant blue R dye adsorption onto meranti wood based activated carbon. *Arab. J. Chem.* 16, 104683.
- Foo, K., Hameed, B.H., 2010. An overview of dye removal via activated carbon adsorption process. *Desalin. Water Treat.* 19 (1–3), 255–274.
- Gayathri, R., Gopinath, K.P., Senthil Kumar, P., Suganya, S., 2019. Adsorption capability of surface-modified jujube seeds for Cd(II) Cu(II) and Ni(II) ions removal: Mechanism, equilibrium, kinetic and thermodynamic analysis. *Desalin. Water Treat.* 140, 268–282.
- Gong, J., Yang, C., Pu, W., Zhang, J., 2011. Liquid phase deposition of tungsten doped TiO<sub>2</sub> films for visible light photoelectrocatalytic degradation of dodecyl-benzenesulfonate. *Chem. Eng. J.* 167 (1), 190–197.
- Haque, E., Lee, J.E., Jang, I.T., Hwang, Y.K., Chang, J.-S., Jegal, J., Jhung, S.H., 2010. Adsorptive removal of methyl orange from aqueous solution with metal-organic frameworks, porous chromium-benzenedicarboxylates. *J. Hazard. Mater.* 181 (1–3), 535–542.
- Hashem, F., 2012. Adsorption of methylene blue from aqueous solutions using Fe<sub>3</sub>O<sub>4</sub>/bentonite nanocomposite. *Hydrology. Current Research* 3 (5).
- Hashem, F., Amin, M., 2016. Adsorption of methylene blue by activated carbon derived from various fruit peels. *Desalin. Water Treat.* 57 (47), 22573–22584.
- He, K., Chen, G., Zeng, G., Chen, A., Huang, Z., Shi, J., Hu, L., 2018. Enhanced removal performance for methylene blue by kaolin with graphene oxide modification. *J. Taiwan Inst. Chem. Eng.* 89, 77–85.
- Katsumata, H., Kobayashi, T., Kaneco, S., Suzuki, T., Ohta, K., 2011. Degradation of linuron by ultrasound combined with photo-Fenton treatment. *Chem. Eng. J.* 166 (2), 468–473.
- Kheraa, R.A., Iqbal, M., Ahmad, A., Hassand, S.M., Nazirb, A., Kausare, A., Kusuma, H.S., Niasrg, J., Masoodh, N., Younasb, U., Nawazi, R., Khan, M.I., 2020. Kinetics and equilibrium studies of copper, zinc, and nickel ions adsorptive removal on to Archontophoenix alexandrae: conditions optimization by RSM. *Desalin. Water Treat.* 201, 289–300.
- Kuncoro, E.P., Soedarti, T., Widialekson, T., Putranto, C., Darmokoesoemo, H., Abadi, N.R., Kusuma, H.S., 2018a. Characterization of a mixture of algae waste-bentonite used as adsorbent for the removal of Pb<sup>2+</sup> from aqueous solution. *Data Brief* 16, 908–913.
- Kuncoro, E.P., Isnadina, D.R.M., Darmokoesoemo, H., Fauziah, O. R., Septya, H., 2018b. Kusuma Characterization, kinetic, and isotherm data for adsorption of Pb<sup>2+</sup> from aqueous solution by adsorbent from mixture of bagasse-bentonite. *Data Brief* 16, 622–629.
- Lazar, M.A., Varghese, S., Nair, S.S., 2012. Photocatalytic water treatment by titanium dioxide: recent updates. *Catalysts* 2 (4), 572–601.
- Liu, T., Li, T., Du, Q., Sun, J., Jiao, Y., Yang, G., Wang, Z., Xia, Y., Zhang, W., Wang, K., 2012. *Colloids Surf. B: Biointerfaces* 90, 19.
- Marcilin, A., Therese, M., Nandhitha, N., 2014. An insight into the selection of nano particle for removing contaminants in waste water. *Int. J. Eng. Res. Appl.* 4 (4), 203–208.
- McDonald, K.J., Reddy, K., Singh, N., Singh, R.P., Mukherjee, S., 2015. Removal of arsenic from groundwater in West Bengal, India using CuO nanoparticle adsorbent. *Environ. Earth Sci.* 73 (7), 3593–3601.
- Memon, G.Z., Moghal, M., Memon, J.R., Memon, N.N., Bhangar, M., 2014. Adsorption of selected pesticides from aqueous solutions using cost effective walnut shells. *Adsorption* 4 (10).
- Miao, L., Wang, C., Hou, J., Wang, P., Ao, Y., Li, Y., You, G., 2017. Response of wastewater biofilm to CuO nanoparticle exposure in terms of extracellular polymeric substances and microbial community structure. *Sci. Total Environ.* 579, 588–597.
- Monteiro-Riviere, N.A., Wiench, K., Landsiedel, R., Schulte, S., Inman, A.O., Riviere, J.E., 2011. Safety evaluation of sunscreen formulations containing titanium dioxide and zinc oxide nanoparticles in UVB sunburned skin: an in vitro and in vivo study. *Toxicol. Sci.* 123 (1), 264–280.
- Mugundan, S., Rajamannan, B., Viruthagiri, G., Shanmugam, N., Gobi, R., Praveen, P., 2015. Synthesis and characterization of undoped and cobalt-doped TiO<sub>2</sub> nanoparticles via sol-gel technique. *Appl. Nanosci.* 5 (4), 449–456.
- Nabi, G., Raza, W., Tahir, M.B., 2020. Green synthesis of TiO<sub>2</sub> nano particle using cinnamon powder extract and the study of optical properties. *J. Inorganic Organometallic Polym. Mater.* 30 (4), 1425–1429.
- Narayana, R.L., Matheswaran, M., Abd Aziz, A., Saravanan, P., 2011. Photocatalytic decolourization of basic green dye by pure and Fe, Co doped TiO<sub>2</sub> under daylight illumination. *Desalination* 269 (1–3), 249–253.
- Neolaka, Y.A., Riwu, A.A., Aigbe, U.O., Ukhurebor, K.E., Onyan-cha, R.B., Darmokoesoemo, H., Kusuma, H.S., 2023. Potential of activated carbon from various sources as a low-cost adsorbent to remove heavy metals and synthetic dyes. *Results Chem.* 5.
- Pascariu, P., Corneliu Cojocar, C., Samoila, P., Airinei, A., Olaru, N., Rotaru, A., Romanitan, C., Tudoran, L.B., Sucheana, M., 2021. Cu/TiO<sub>2</sub> composite nanofibers with improved photocatalytic performance under UV and UV-visible light irradiation. *J. Surf. Sci.* 2021.
- Patrick, J.W., 1995. *Porosity in Carbons: Characterization and Applications*. Edward Arnold.
- Pearce, C., Lloyd, J., Guthrie, J., 2003. The removal of colour from textile wastewater using whole bacterial cells: a review. *Dyes Pigm.* 58, 179–196.
- Pérez-González, A., Urtiaga, A., Ibáñez, R., Ortiz, I., 2012. State of the art and review on the treatment technologies of water reverse osmosis concentrates. *Water Res.* 46 (2), 267–283.
- Pichot, F., Pitts, J.R., Gregg, B.A., 2000. Low-temperature sintering of TiO<sub>2</sub> colloids: application to flexible dye-sensitized solar cells. *Langmuir* 16 (13), 5626–5630.
- Rida, K., Bouraoui, S., Hadnine, S., 2013. Adsorption of methylene blue from aqueous solution by kaolin and zeolite. *Appl. Clay Sci.* 83–84, 99–105. <https://doi.org/10.1016/j.clay.2013.08.015>.
- Sadanandam, G., Lalitha, K., Kumari, V.D., Shankar, M.V., Subrahmanyam, M., 2013. Cobalt doped TiO<sub>2</sub>: a stable and efficient photocatalyst for continuous hydrogen production from glycerol:

- Water mixtures under solar light irradiation. *Int. J. Hydrogen Energy* 38 (23), 9655–9664.
- Shahmoradi, B., Ibrahim, I.A., Sakamoto, N., Ananda, S., Somashekar, R., Row, T.N.G., Byrappa, K., 2010. Photocatalytic treatment of municipal wastewater using modified neodymium doped TiO<sub>2</sub> hybrid nanoparticles. *J. Environ. Sci. Health A* 45 (10), 1248–1255.
- Sohrabnezhad, S., Pourahmad, A., Rakhshae, R., Radaee, A., Heidarian, S., 2010. Catalytic reduction of methylene blue by sulfide ions in the presence of nanoAlMCM-41 material. *Superlattice. Microst.* 47 (3), 411–421.
- Sushma, D., Richa, S., 2015. Use of nanoparticles in water treatment: a review. *Int. Res. J. Environ. Sci* 4 (10), 103–106.
- Tepuš, B., Simonič, M., Petrinić, I., 2009. Comparison between nitrate and pesticide removal from ground water using adsorbents and NF and RO membranes. *J. Hazard. Mater.* 170 (2–3), 1210–1217.
- Üner, O., Geçgel, Ü., Bayrak, Y., 2016. Adsorption of methylene blue by an efficient activated carbon prepared from *Citrullus lanatus* rind: kinetic, isotherm, thermodynamic, and mechanism analysis. *Water Air Soil Pollut.* 227 (7), 1–15.
- Van der Bruggen, B., Milis, R., Vandecasteele, C., Bielen, P., Van San, E., Huysman, K., 2003. Electrodialysis and nanofiltration of surface water for subsequent use as infiltration water. *Water Res.* 37 (16), 3867–3874.
- Veréb, G., Ambrus, Z., Pap, Z., Kmetykó, Á., Dombi, A., Danciu, V., Mogyorósi, K., 2012. Comparative study on UV and visible light sensitive bare and doped titanium dioxide photocatalysts for the decomposition of environmental pollutants in water. *Appl. Catal. A* 417, 26–36.
- Wu, R., Qu, J., 2005. Removal of water-soluble azo dye by the magnetic material MnFe<sub>2</sub>O<sub>4</sub>. *J. Chem. Technol. Biotechnol.: Int. Res. Process Environ. Clean Technol.* 80 (1), 20–27.
- Yu, J.C., Ho, W., Yu, J., Yip, H., Wong, P.K., Zhao, J., 2005. Efficient visible-light-induced photocatalytic disinfection on sulfur-doped nanocrystalline titania. *Environ. Sci. Tech.* 39 (4), 1175–1179.
- Ziemkowska, W., Basiak, D., Kurtycz, P., Jastrzębska, A., Olszyna, A., Kunicki, A., 2014. Nano-titanium oxide doped with gold, silver, and palladium—synthesis and structural characterization. *Chem. Pap.* 68 (7), 95.